

## A SIMPLE METHOD FOR IONIC AND MOLECULAR ADSORPTION ELECTRICAL CALCULATIONS

J. ROSS MACDONALD and C. A. BARLOW, Jr.

*Texas Instruments Incorporated, Dallas, Texas, U.S.A.*

Received 22 December 1965. Revised manuscript received 11 February 1966

The usual methods for calculating potentials and fields arising from a regular, adsorbed plane array of ions or dipoles are complex and time consuming to apply. We present here a method based on a modification of Grahame's cut-off model which allows several such quantities to be calculated accurately but rapidly from simple closed formulas. The method is applied to hexagonal arrays of ideal and non-ideal dipoles. Non-ideal dipoles are assumed to arise from imaging of an array of adions in a conducting adsorbent. Results of the simple, approximate formulas are compared in detail with very accurate results obtained from lengthy computer calculations. We believe the latter will be unnecessary hereafter, whenever the field or potential is desired on a line perpendicular to the plane adsorbent through a removed dipole or ion. With proper normalization, potential-distance curves for ideal and non-ideal (finite-length) dipoles are found to be nearly the same. Finally, the present results are employed to yield an improved formula for the change of work function of a conducting surface, when a hexagonal array of polarizable molecules or atoms is adsorbed on it. The formula is illustrated and shows that adsorbed uncharged elements, with sufficiently high but still physical polarizability, must either ionize or their polarizability decrease upon adsorption.

### 1. Introduction

Consider a fixed, planar, hexagonal array of infinite extent made up of either discrete ideal dipoles or of adsorbed ions and their images in a conducting plane adsorbent (non-ideal dipoles). Calculation of the work of adsorption or desorption of an array element requires knowledge of the electric field,  $\mathcal{E}$ , and electrostatic potential,  $\psi$ , along an outward perpendicular to the surface, ( $+z$  direction) taken through the position of a missing array element. We have elsewhere calculated this field and potential very accurately for arrays of non-polarizable non-ideal dipoles<sup>1</sup>). In addition, we have recently given somewhat more approximate expressions for electron<sup>2</sup>) and ionic work functions<sup>3</sup>) for an array of polarizable ions and their images. All these calculations require computation of  $\mathcal{E}$  and  $\psi$  as functions of  $z$  and of lattice spacing  $r_1$ , where  $r_1$  is the nearest neighbor distance of a hexagonal array. Here, we shall develop relatively simple expressions for  $\mathcal{E}$  and  $\psi$ , appropriate for both ideal and non-ideal dipole arrays. Their relatively high

accuracy and simplicity expedite calculations of the type cited above greatly. The problem of stability of the hexagonal array and thermal disordering has been examined elsewhere<sup>4</sup>); here, we assume the array is rigid, a useful approximation in many cases of experimental interest for adsorption from either a gas or liquid phase.

In 1927 Topping<sup>5</sup>), in a much cited paper, calculated the mutual potential energy of a plane, hexagonal array of ideal, non-polarizable dipoles. His result may be readily transformed to yield the field at the position of a removed dipole

$$\mathcal{E} = \mathcal{E}_I(0) = -\sigma\mu r_I^{-3}, \quad (1)$$

where the subscript *I* denotes ideal dipoles,  $\mu$  is the dipole moment of a discrete dipole, and  $\sigma \cong 11.0341754$ , a number derived from a lattice sum<sup>5,6</sup>). Although Topping's treatment cannot be used to calculate the field accurately at a distance  $z > 0$  in front of the plane of dipoles, it furnishes an accurate value to which any more general result should reduce for  $z = 0$ , the plane of the dipoles. Even though the above expression applies for an array of ideal dipoles having fixed moments  $\mu$ , it may be easily modified for polarizable ideal dipoles<sup>2,7,8</sup>). In most of the present treatment, ions and dipoles will be taken non-polarizable, however, since polarization modifications have been recently discussed<sup>2,3</sup>) and require expressions for  $\mathcal{E}$  and  $\psi$  such as those derived herein.

In the following section, formulas for  $\mathcal{E}$  and  $\psi$  will be derived for ideal dipoles by modifying a known approach appropriately, then the results extended to arrays of non-ideal dipoles consisting, for example, of ions and their images. Next, an evaluation of the accuracy of the present results will be presented by comparing them with those accurately calculated from a very complex lattice-sum approach<sup>1</sup>). Finally, we will use the present results to calculate the potential change arising from an adsorbed array of ideal dipoles.

## 2. Derivation of formulas

Grahame<sup>9</sup>) seems to have been the first to introduce a cut-off model for calculating approximate fields and potentials of the present type. The model does not allow calculation of the field and potential anywhere but along the perpendicular line through a removed array element, an adion or ideal dipole. Calculations for other positions require a lattice-sum approach<sup>1</sup>). For the discrete ideal dipole case, the actual discrete distribution is replaced in the cut-off approximation by a uniform dipole sheet containing a circular vacancy of radius  $r_0$ . For Grahame's non-ideal dipole case, he actually used a radius which led to a removed circular hole of area just containing the

charge of a single adion and its image. Let  $N$  be the number per unit area of adions or discrete ideal dipoles. Note that  $N$  may be written as  $\theta N_s$ , where  $0 \leq \theta \leq 1$  and  $N_s$  is the full monolayer coverage. For a hexagonal lattice  $N = (\frac{4}{3}r_1^{-4})^{\frac{1}{2}}$ , and Grahame's choice of  $r_0$  may be written as  $r_0 = r_{0G} \equiv (\pi N)^{-\frac{1}{2}} = (\sqrt{3}/2\pi)^{\frac{1}{2}}r_1 \cong 0.525\ 037\ 6\ r_1$ . Although this expression for  $r_0$ , which has been used by several authors<sup>10-13</sup>) since Grahame, seems intuitively plausible, we shall see that while it is a fairly good approximation for the hexagonal lattice over the experimental ranges of  $z$  and  $r_1$  of interest, it is only exact for a fixed lattice in the limits  $r_1 \rightarrow 0$  or  $z \rightarrow \infty$ . When thermal agitation is important, it may, however, be more appropriate in some circumstances than the following fixed hexagonal approach.

For a uniform, smeared ideal dipole layer of strength  $N\mu$  per unit area, the potential for  $z > 0$  is

$$\psi_\infty = 2\pi N\mu \tag{2}$$

and is positive when the positive pole is toward the  $+z$  direction. Let  $\xi \equiv z/r_1$  and calculate the potential arising from the ideal-dipole cut-off model at a position  $z$  along the perpendicular line through the center of the circular vacancy. This potential is easily obtained by integration and is

$$\begin{aligned} \psi_1(\xi) &= (2\pi N\mu) [z/(z^2 + r_0^2)^{\frac{1}{2}}] \\ &= \psi_\infty / [1 + (p/\xi)^2]^{\frac{1}{2}}. \end{aligned} \tag{3}$$

Note that  $\psi_1(\xi)/\psi_\infty$  is only a function of  $\xi$ , not of  $z$  and  $r_1$  separately. We have written  $p \equiv r_0/r_1$  in (3).  $\psi_1(\xi)$  goes to  $\psi_\infty$  as it should for fixed  $z$  and  $r_0 \rightarrow 0$  and for fixed  $r_0$ ,  $z \rightarrow \infty$ .

Grahame's choice of  $r_0$  leads to  $p = p_G \equiv p_\infty = (\sqrt{3}/2\pi)^{\frac{1}{2}} \cong 0.5250376$ , where the subscript  $\infty$  refers to the limit  $\xi \rightarrow \infty$ . Although eq. (3) with  $p = p_\infty$  is approximate for a hexagonal array situation except when  $\xi \rightarrow \infty$ , this equation can be made exact when  $p$  is made the appropriate function of  $\xi$ . Approximations to the  $p(\xi)$  which makes (3) exact will now be developed. The value of this approach is that  $p$  also appears in the formulas for the non-ideal dipole situation and even there the  $p(\xi)$  derived from the ideal dipole case turns out to be a good approximation. Although the  $p$  for the non-ideal dipole case is a function of  $R_1$  (see following definition) as well as  $\xi$ , the  $R_1$  dependence is very slight and as, we shall see, may frequently be neglected entirely.

Although  $p_\infty$  is the smallest value appropriate for a fixed hexagonal lattice, we show elsewhere<sup>14</sup>) that the mean distance of nearest neighbors for a random array without interactions between its elements is  $(4N)^{-\frac{1}{2}}$ . This corresponds to  $p \cong 0.465$ , if  $r_0$  is taken as the mean nearest-neighbor separation distance and  $r_1$  is defined by  $(\frac{4}{3})^{\frac{1}{2}}N^{-\frac{1}{2}}$  as for a hexagonal array. For a somewhat disordered array with repulsive interactions,  $p$  must exceed the

value appropriate without interactions, in agreement with the strong interaction, fixed hexagonal array result  $p_\infty \cong 0.525\ 037\ 6$ . It is next of value to obtain the maximum possible value of  $p$  for a rigid hexagonal array. Since  $\mathcal{E}_1(\xi) = -r_1^{-1} (d\psi_1/d\xi)$ , eq. (3) with  $p = p(\xi)$  leads to

$$\mathcal{E}_1(\xi) = -\frac{(\psi_\infty/r_1)(1+F)}{p[1+(\xi/p)^2]^{\frac{3}{2}}}, \quad (4)$$

where  $F(\xi) \equiv -d \ln p(\xi)/d \ln \xi$ . We shall find that  $p(\xi)$  varies only slowly with  $\xi$  and that  $F(\xi) = 0$  for  $\xi = 0$ . Then, writing  $p(0) \equiv p_0$ , we have

$$\mathcal{E}_1(0) = -\psi_\infty/r_1 p_0. \quad (5)$$

On setting eqs. (1) and (5) equal, we obtain  $p_0 \equiv 4\pi/\sqrt{3}\sigma \cong 0.657\ 520\ 592$ , showing that  $p$  only changes from about 0.53 to 0.66 as  $\xi$  varies from  $\infty$  to zero. The present value of  $p_0$  has been used for all  $\xi$  in some of the earlier work of the present authors<sup>2,3</sup>) in preference to  $p_\infty$ , since higher accuracy is attained thereby in experimental ranges of interest and since the choice of  $p_0$  leads properly to ideal dipole results in the limit that non-ideal dipole arrays degenerate to ideal dipole arrays. As we shall show, much higher accuracy for both ideal and non-ideal dipole arrays can be obtained by using a variable  $p(\xi)$  than by using a constant  $p$ , however. Thus, the accuracy of the results given in refs. 2) and 3) can be appreciably improved by using the present formulations in appropriate equations.

In order to obtain the  $p(\xi)$  function which makes eq. (3) exact for a hexagonal array, we need accurate values of  $\psi_1(\xi)$ . These can be obtained from our previous non-ideal dipole lattice-sum calculation<sup>1</sup>). Let  $\beta$  be the distance between the charge centroid of an adion and the imaging plane of the adsorbent electrode ( $z=0$ ). The dipole moment of the adion-image pair is then  $\mu = 2z_v e\beta$ , where  $z_v$  is the effective valence of the adsorbed ion. The average charge density,  $q_a$ , is then just  $z_v eN$ . We take the electrode grounded here so its charge density is just  $-z_v eN$  and  $\psi_\infty = 4\pi N z_v e\beta$ . It will be convenient to define the normalized variables  $R_1 \equiv r_1/\beta$  and  $Z \equiv z/\beta$ . Then,  $\xi = Z/R_1 \equiv z/r_1$  remains unchanged. Note that  $R_1 = 2$  is the minimum possible value allowed by steric restrictions for spherical adions having their charge centroids at the sphere center. Smaller values of  $R_1$  will therefore usually not need to be considered. If the minimum value of  $R_1$  (corresponding to a full monolayer) is denoted as  $R_{1m}$ , then  $R_1 = 0^{-\frac{1}{2}} R_{1m}$ .

Although the results of the exact lattice-sum treatment<sup>1</sup>) are quite complex in the general case, they reduce to

$$\frac{\psi_N(Z, R_1)}{\psi_\infty} = 1 - \left(\frac{\sqrt{3}}{4\pi}\right) \left(\frac{R_1^2}{Z^2 - 1}\right) \quad (6)$$

and

$$\frac{\mathcal{E}_N(Z, R_1)}{\mathcal{E}_\infty} = \left(\frac{\sqrt{3}}{2\pi}\right) \left(\frac{ZR_1^2}{(Z^2 - 1)^2}\right) \tag{7}$$

for  $Z \geq 1 + 3R_1$ . Here the subscript N refers to non-ideal, and these equations hold to one part in  $10^8$  or better. The quantity  $\mathcal{E}_\infty$  is  $-\psi_\infty/\beta = -4\pi Nz_v e$ . Now if we express (6) and (7) in terms of  $\xi$  wherever possible and then let  $R_1 \rightarrow \infty$ , while keeping  $\xi$  fixed, we obtain

$$\frac{\psi_1(\xi)}{\psi_\infty} = 1 - \left(\frac{\sqrt{3}}{4\pi}\right) \xi^{-2} \quad (\xi \geq 3), \tag{8}$$

$$\mathcal{E}_1(\xi) = -\left(\frac{\sqrt{3}}{2\pi}\right) \left(\frac{\psi_\infty}{r_1}\right) \xi^{-3} \quad (\xi \geq 3), \tag{9}$$

where  $4\pi Nz_v e\beta$  has been replaced by  $\psi_\infty = 2\pi N\mu$  in (9). Such replacement is justified since  $R_1$  may approach infinity by  $\beta$  approaching zero but keeping  $\mu = 2z_v e\beta$  a constant. Since eqs. (8) and (9) are exceedingly accurate for  $\xi \geq 3$ , we now need to obtain  $p(\xi)$  only in the range  $0 < \xi < 3$ .

To obtain accurate results for  $\psi_1(\xi)$  in the region  $0 < \xi < 3$ , accurate values of  $\psi_N(Z, R_1)/\psi_\infty$  were first obtained<sup>1)</sup> for given  $\xi$  values for  $R_1 = 50, 100$  and  $200$ . They were nearly equal but were extrapolated to  $R_1 = \infty$  using the epsilon algorithm<sup>15)</sup>. The resulting values of  $\psi_1(\xi)/\psi_\infty$  were then used together with (3) to calculate accurate values of  $p(\xi)$ .

In the non-ideal dipole case, the cut-off model leads to<sup>1)</sup>

$$\psi_N(Z, R_1)/\psi_\infty = \frac{1}{2} \{ [(pR_1)^2 + (Z + 1)^2]^{\frac{1}{2}} - [(pR_1)^2 + (Z - 1)^2]^{\frac{1}{2}} \}. \tag{10}$$

For a given  $R_1$ , (10) may be used together with accurate values of  $\psi_N/\psi_\infty$  to calculate  $p(\xi)$ . We have done so for  $R_1 = 2, 3$  and  $5$  for comparison with the  $R_1 = \infty$  ideal-dipole-layer results. The four curves of  $p(\xi)$  are shown in fig. 1 on an expanded ordinate scale. It will be seen that even the curve for  $R_1 = 2$  is very close to that for  $R_1 = \infty$  over most of the  $\xi$  range. This range is here extended to  $3.5$  since the condition  $Z \geq 1 + 3R_1$  leads to  $\xi \geq 3.5$  when  $R_1 = 2$ , usually the smallest value of  $R_1$  that need be considered. Note that although the  $\xi = 0$  values of  $p(\xi)$  are unequal to  $p_0$  for  $R_1 < \infty$ , the deviation is quite small even for  $R_1 = 2$ . When  $p$  is taken as a function of  $\xi$  in (10), the corresponding non-ideal-dipole layer field is

$$\frac{\mathcal{E}_N(Z, R_1)}{\mathcal{E}_\infty} = \frac{1}{2} \left\{ \frac{Z + 1 - [(pR_1)^2/Z] F}{[(pR_1)^2 + (Z + 1)^2]^{\frac{1}{2}}} - \frac{Z - 1 - [(pR_1)^2/Z] F}{[(pR_1)^2 + (Z - 1)^2]^{\frac{1}{2}}} \right\}, \tag{11}$$

a result which reduces properly to (4) when  $R_1 \rightarrow \infty$  and  $\mu$  and  $\xi$  are held fixed.

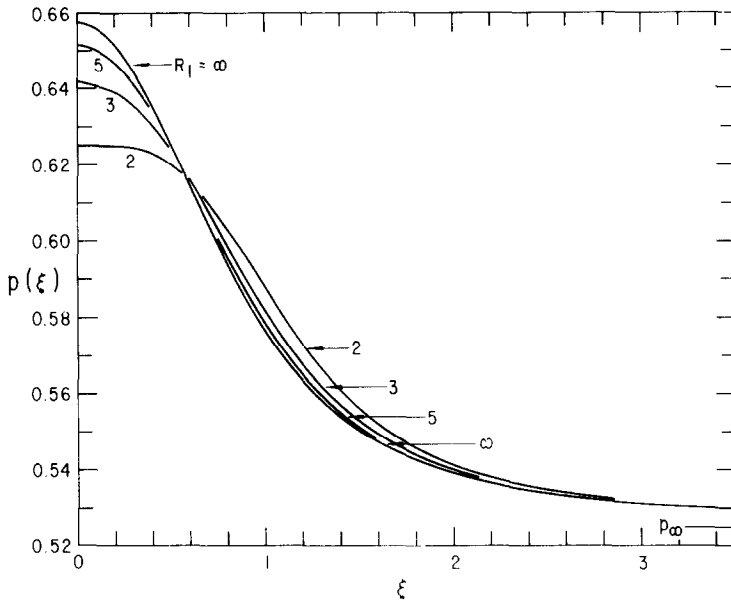


Fig. 1. The function  $p(\xi)$  for  $R_1 = 2, 3, 5$  and  $\infty$  (ideal dipoles) plotted with an expanded ordinate scale.

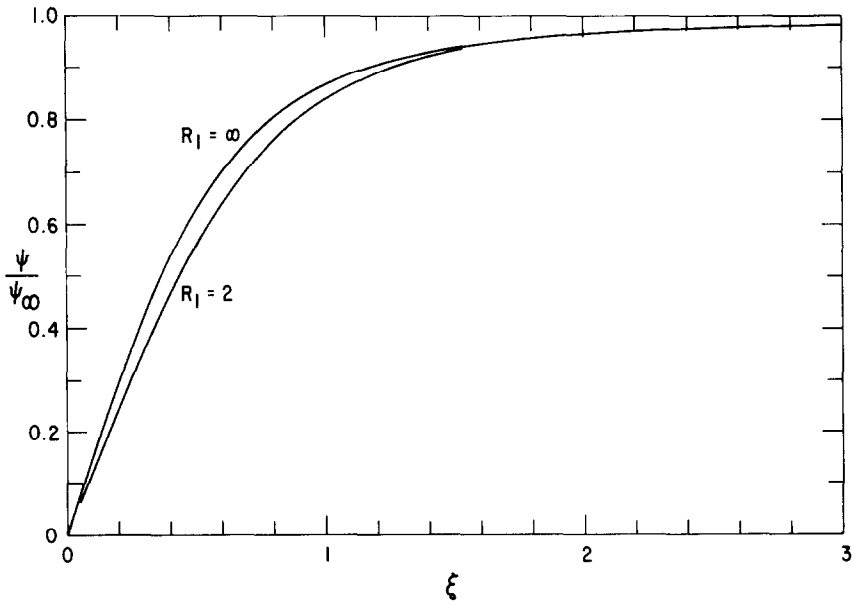


Fig. 2. The normalized potential  $\psi/\psi_\infty$  vs.  $\xi$  for  $R_1 = 2$  and  $\infty$ .

Fig. 2 shows accurately calculated curves of normalized potential in the ideal dipole case,  $\psi_I/\psi_\infty$ , and in the non-ideal dipole case,  $\psi_N/\psi_\infty$ . For the latter curve, the minimum value  $R_1=2$  was used, while  $R_1=\infty$  in the ideal dipole situation. The relatively small difference between the curves of course explains why  $p(\xi)$  is only a weak function of  $R_1$  ( $2 \leq R_1 < \infty$ ) as illustrated in fig. 1. It has not usually been recognized that the use of the variable  $\xi$  rather than  $Z$  or  $z$  tremendously reduces the explicit dependence of  $\psi/\psi_\infty$  curves on  $R_1$ . Thus, widely spread families of curves calculated in an approximate fashion have been given for finite dipoles<sup>16,17</sup>) and a similar set of curves has been calculated for ideal dipoles<sup>17</sup>), even though in the latter case they all degenerate to a single one when  $\xi$  instead of  $z$  is used as independent variable. Although all of the preceding results are based on the assumption of a hexagonal lattice, Swanson and Gomer<sup>16</sup>) and the authors<sup>8</sup>) have pointed out that virtually the same potentials are obtained for a square array of the same surface density as a given hexagonal array.

Although only  $p(\xi, R_1)$  is needed to calculate potentials accurately, its associated function  $F(\xi, R_1)$  is required as well for field calculation. Since  $F$ , like  $p$ , is relatively independent of  $R_1$  ( $2 \leq R_1 \leq \infty$ ), reaches a maximum of only about 0.14 near  $\xi = 1$ , and decreases continuously for smaller or larger  $\xi$ , it may frequently be neglected compared to unity. Although  $F$  may be obtained from  $p$  by differentiation, we have found it more convenient to obtain it from eqs. (4) and (11) by using accurate values of the field ratios and the appropriate accurate  $p$  values.

### 3. Explicit approximation results

Although the accurate curves of  $p(\xi)$  presented in fig. 1 allow quite accurate calculations of  $\psi/\psi_\infty$  to be made for given values of  $Z$  and  $R_1$  (or  $z$  and  $r_1$ ), frequently both fields and potentials are required for many  $Z$  and  $R_1$  combinations. It is then desirable to have entirely analytic expressions available for hexagonal array potentials and fields. In this section, we shall thus discuss analytic approximations to  $p(\xi, R_1)$  and  $F(\xi, R_1)$  for  $R_1=2, 5$  and  $\infty$ , and will use these to calculate  $\psi/\psi_\infty$  and  $\mathcal{E}/\mathcal{E}_\infty$  for various  $R_1$  values for comparison with accurate values of these ratios. The resulting standard errors will show how good the several analytic forms are for calculating  $\psi/\psi_\infty$ , for example.

The simplest calculations of  $\psi_I/\psi_\infty$  and  $\psi_N/\psi_\infty$  use a constant value of  $p$ . Table 1 lists the standard errors obtained for  $p \cong p_\infty$ ,  $p \cong p_0$ , and the non-linear least-squares values of  $p$  shown, for several values of  $R_1$ . Here, constant values of  $p$  were used in eqs. (3) ( $R_1=\infty$ ) and (10) (for  $R_1=2, 3, 5$  and 10) to fit sets of 27 accurate potential ratios covering the range

TABLE 1  
Standard error values for fitting of  $\psi_N/\psi_\infty$  and  $\psi_1/\psi_\infty$  using constant values of  $p$

$R_1$	$p = 0.525\ 0376 \cong p_\infty$	Least-squares $p$	$p = 0.657\ 520\ 59 \cong p_0$
2	0.024 01	0.007 062 ( $p \cong 0.599\ 193$ )	0.018 83
3	0.028 22	0.008 834 ( $p \cong 0.603\ 976$ )	0.019 47
5	0.031 19	0.010 08 ( $p \cong 0.607\ 183$ )	0.019 86
10	0.032 69	0.010 69 ( $p \cong 0.608\ 752$ )	0.020 04
$\infty$	0.033 24	0.010 91 ( $p \cong 0.609\ 308$ )	0.020 10

$0 \leq \xi \leq 3.5$  for each  $R_1$  value. As table 1 indicates,  $p_0$  yields a slightly better fit than  $p_\infty$ , and the least-squares values are about a factor of two better than those using  $p_0$ . Note that since the least-squares values vary only slightly with  $R_1$ , a best-choice value of  $p$  for all  $R_1$  values of interest would be about 0.607. For many purposes, sufficient accuracy in calculating values of  $\psi/\psi_\infty$  will be achieved using just this value throughout the calculation.

There are instances where the accuracy illustrated in table 1 is insufficient. In particular, as we show elsewhere<sup>18</sup>, values of  $\psi/\psi_\infty$  and  $\mathcal{E}/\mathcal{E}_\infty$  can be used to obtain partial and infinite imaging potentials and fields. In such situations, an adion may be partly or completely imaged by another plane parallel to but separated from the electrode in addition to its imaging in the electrode. Such behavior is particularly important for adsorption from electrolyte solutions and frequently requires quite accurate values of the present  $\psi/\psi_\infty$  ratios to yield sufficient accuracy in the final potentials.

In order to deal with situations where constant  $p$  yields insufficient accuracy, we have chosen to represent  $p$  and  $F$  by rational function approximations of the Chebyshev type, which minimize the absolute value of the relative (or absolute) error between accurate functional values and those given by the approximation. In the appendix, coefficients of the polynomials entering the approximation formulas for  $p$  and  $F$  are given. For the more important  $p$ , we present both linear/linear (1/1) and quadratic/quadratic (2/2) approximations for  $R_1 = 2, 5$  and  $\infty$ . For  $F$  only the simplest linear/quadratic (1/2) approximation is included.

Table 2 shows the small standard errors which result when  $\psi/\psi_\infty$  is calculated using the (1/1) and (2/2) approximations to  $p(\xi)$ . The vertical column  $R_1$  values denote those  $R_1$ 's used in calculating the exact data with which the approximate results were compared, while the top horizontal  $R_1$ 's indicate the values of  $R_1$  associated with the approximations to  $p(\xi)$  used



TABLE 2  
Standard error values for fitting of  $\psi_N/\psi_\infty$  and  $\psi_I/\psi_\infty$  using variable values of  $p$

$R_1$	$p(\xi)$ approximations for $R_1 = 2$		$p(\xi)$ approximations for $R_1 = 5$		$p(\xi)$ approximations for $R_1 = \infty$	
	(1/1)	(2/2)	(1/1)	(2/2)	(1/1)	(2/2)
2	$2.720 \times 10^{-3}$	$2.088 \times 10^{-4}$	$2.325 \times 10^{-3}$	$2.600 \times 10^{-3}$	$2.834 \times 10^{-3}$	$3.109 \times 10^{-3}$
3	$3.859 \times 10^{-3}$	$1.902 \times 10^{-3}$	$2.406 \times 10^{-3}$	$1.128 \times 10^{-3}$	$2.351 \times 10^{-3}$	$1.723 \times 10^{-3}$
5	$4.890 \times 10^{-3}$	$3.273 \times 10^{-3}$	$2.903 \times 10^{-3}$	$1.071 \times 10^{-4}$	$2.323 \times 10^{-3}$	$7.262 \times 10^{-4}$
10	$5.441 \times 10^{-3}$	$3.960 \times 10^{-3}$	$3.240 \times 10^{-3}$	$4.702 \times 10^{-4}$	$2.420 \times 10^{-3}$	$2.329 \times 10^{-4}$
$\infty$	$5.643 \times 10^{-3}$	$4.206 \times 10^{-3}$	$3.370 \times 10^{-3}$	$6.580 \times 10^{-4}$	$2.472 \times 10^{-3}$	$8.105 \times 10^{-5}$

in the formulas. The standard error results shown in tables 1 and 2 indicate that all the (1/1) approximations lead to standard errors roughly an order of magnitude smaller than those obtained with constant  $p_0$  or  $p_\infty$  and around three times lower than the constant least-squares values of  $p$ . The (2/2) approximations lead to far smaller standard errors than the (1/1) ones when the  $R_1$  of the approximation is near the  $R_1$  of the comparison data. When this is not the case, the (2/2) approximations are only slightly superior to the (1/1)'s. Since  $R_1 = 5$  is near the middle of the range of usual interest, the (1/1)  $R_1 = 5$  approximation for  $p(\xi)$  will usually be sufficiently accurate for any value of  $R_1$  in the range  $2 \leq R_1 < \infty$ . Note that  $R_1 = 5$  corresponds to  $q_a \cong 18.5 \mu\text{C}/\text{cm}^2$  and to  $N \cong 1.15 \times 10^{14} \text{cm}^{-2}$  when  $\beta = 2\text{\AA}$  and  $z_v = 1$ . The above formulas and the expressions for  $p$  and  $F$  may now be directly applied, as illustrated in the next section, to the calculation of the electrical effects of adsorbed arrays of ions, atoms, or molecules.

#### 4. Work function change on dipolar adsorption

An old problem of continuing interest is the calculation of the change in electron average work function,  $\Delta V$ , when a discrete array of identical dipoles is adsorbed on a conducting surface. The individual dipoles may be polarizable molecules with a permanent dipole moment, and/or dipoles induced in polarizable atoms or molecules by a "natural" surface field<sup>8)</sup>  $\mathcal{E}_{n1}$  and/or a surface charge density  $q$ . For simplicity, we shall here consider that the dipoles are ideal, the polarizability  $\alpha$  is independent of field, and that the orientation of any permanent dipoles remains unchanged as the field changes (we take all such dipoles lined up perpendicular to the adsorbent plane).

The common solutions to the above problem<sup>8)</sup> are sometimes useful, but are so overly approximate as to be frequently very misleading. In particular, discreteness of the dipole array itself is often neglected and the effects of imaging of the dipoles themselves are almost invariably omitted. These effects, which affect the induced polarization, may be of great importance whenever the atom or molecule is polarizable, as all real atoms and molecules are.

The steps involved in a correct solution to the above problem, one which includes the usually omitted factors, may be skipped here since they appear in refs. <sup>2)</sup> and <sup>8)</sup>. On combining eq. (19) of ref. <sup>8)</sup> and eq. (17) of ref. <sup>2)</sup>, we have, after minor changes,

$$\Delta V = V(\mathcal{P}) - V(0) = -4\pi N [\alpha(4\pi q + \mathcal{E}_{n1}) + \mu_0] / \epsilon_1, \quad (12)$$

$$\epsilon_1 \equiv 1 + J \left[ \sigma R_1^{-3} - \frac{1}{4} + \left( \frac{\pi}{2\sqrt{3}} \right) \frac{\{p^2(1+F)\}}{\{1+(p/\xi)^2\}^{\frac{3}{2}}} \right], \quad (13)$$

where  $\mu_0$  is the permanent moment (if any) of an adsorbed molecule, or its invariant component perpendicular to the surface. In eq. (12),  $\mathcal{P}$  is the average polarization of the dipole array, and thus  $\Delta V$  refers to the potential arising from the array minus that without it. The work function of the bare surface does not, therefore, appear in  $\Delta V$ . Note that when  $q=0$ ,  $\Delta V = -\psi_\infty$ , where  $\psi_\infty$  is, as usual, the potential (referred to zero at the electrode) a large distance in front of the adsorbent and its array.

The principal new terms appear in eq. (13) for the effective dielectric constant. Here  $J \equiv \alpha/\beta^3$ , where  $\beta$  is now the distance between the electrical centers of adsorbed dipoles and the conducting, imaging surface. The separation  $\beta$  might, for example be roughly the radius of an adatom. Its introduction allows us to again use  $R_1 \equiv r_1/\beta \equiv \theta^{-1/2} R_{1m}$  and thus introduce the coverage  $\theta$ . The  $\sigma R_1^{-3}$  term in (13) arose from all the array dipoles surrounding (and in the plane with) a given one and takes into account their polarizing field at the selected one. The next term, involving the number  $\frac{1}{2}$ , appears when one includes the image of the selected dipole, and the last term in (13) accounts for the polarizing field at the given dipole arising from all the array *image* dipoles except that of the selected dipole. This last term has been written in the notation of the present paper and follows immediately from eq. (4). It involves  $\xi$  directly and through the  $p(\xi)$  and  $F(\xi)$  appropriate for ideal dipoles ( $R_1 = \infty$ ). Since here the position we require the field at is a perpendicular distance  $2\beta$  in front of the (image) dipole array,  $\xi = 2\beta/r_1 \equiv 2/R_1$  in (13). Note that if  $R_{1m}$  is taken as 2, then  $\theta = 4/R_1^2 = \xi^2$ . The effective dielectric constant may then be considered a function of  $R_1$ ,  $\xi$  or  $\theta$ .

The present solution for  $\Delta V$  is a completely self-consistent one and has some interesting properties. The most striking is that when  $\xi=0$ ,  $\epsilon_1$  is zero when  $J=4$ . For  $J>4$ , non-physical poles in  $\Delta V$  occur for small positive  $\xi$ 's. This means that a linear theory such as the present one where  $\alpha$  is taken field independent is actually inapplicable for any atom or molecule for which  $J \geq 4$ . For some atoms, such as cesium, the expected  $J$  may apparently be greater than 4. Using the highest value of  $\alpha$  for cesium quoted by De Boer<sup>19)</sup> and Pauling's<sup>20)</sup> value for the radius of a cesium atom, we find  $J \approx 61 \text{ \AA}^3 / (2.35 \text{ \AA})^3 \approx 4.7$ . A value for  $\alpha$  as large as  $67.7 \text{ \AA}^3$  has been calculated theoretically for cesium<sup>21)</sup>. Even when an  $\alpha$  as small as  $50 \text{ \AA}^3$  is used<sup>21)</sup>, it would require only a very small displacement (arising from the attractive dipole-dipole image field) of the dipole centroid from the center of a cesium atom for  $\beta$  to be reduced from  $2.35 \text{ \AA}$  enough for  $J$  to equal or exceed 4. For any adsorbed element for which we might expect  $J \geq 4$  in the adsorbed state, we must either conclude that the atom or molecule in question becomes wholly or partly ionized on adsorption, or that the high fields polarizing the discrete element reduce its polarizability sufficiently that the above catastrophe does

not happen. This failure of linear polarization theory has appeared as a result of properly including the image effects so often entirely neglected. We plan to present elsewhere a treatment of such nonlinear effects.

Using the present ideal dipole ( $R_1 = \infty$ ) rational function approximations for  $p$  and  $F$ , we may readily calculate  $\Delta V$ . On introducing the hexagonal-array relation between  $N$  and  $r_1$ , eqs. (12) and (13) expressed entirely in terms of the variable  $\xi$  become

$$\Delta V = - (2\pi\xi^2/\sqrt{3}\epsilon_1) [J\beta(4\pi q + \epsilon_{n1}) + (\mu_0/\beta^2)], \tag{14}$$

and

$$\epsilon_1 = 1 + J \left[ (\sigma/8)\xi^3 - \frac{1}{4} + \left( \frac{\pi}{2\sqrt{3}} \right) \frac{\{p(\xi)\}^2 \{1 + F(\xi)\}}{[1 + \{p(\xi)/\xi\}^2]^{\frac{1}{2}}} \right]. \tag{15}$$

For the purposes of calculation, we shall choose  $R_{1m} = 2$ , so that  $\theta = \xi^2$ . For any other choice of  $R_{1m}$ , we need only multiply the  $R_{1m} = 2$   $\theta$ -scale values by  $(\frac{1}{2}R_{1m})^2$ . In fig. 3, we present some curves of the normalized

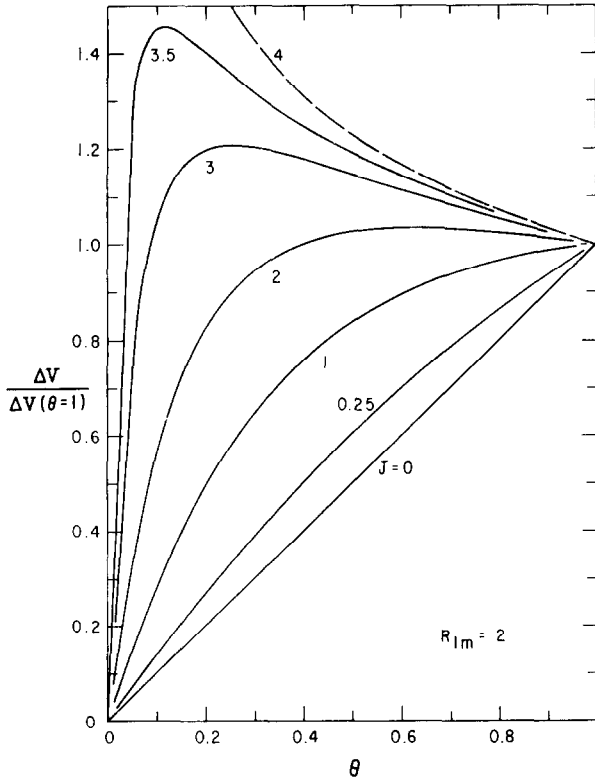


Fig. 3. The normalized electron work function change on ideal dipole adsorption,  $\Delta V/\Delta V(\theta = 1)$ , vs.  $\theta$  for  $R_{1m} = 2$ .

ratio  $\Delta V/\Delta V(\theta=1)=\theta\varepsilon_1(\theta=1)/\varepsilon_1$  for several values of  $J$ . These were calculated using the (1/2) expression for  $F$  and, for highest accuracy, a (3/3) expression<sup>18)</sup> for  $p$ . The dashed  $J=4$  curve is non-physical and represents the envelope of allowable curves.

Although the curves of fig. 3 are of the general form frequently found for adsorption of such materials as cesium or potassium on tungsten<sup>2, 8, 22)</sup>, we shall not carry out detailed fitting of theory and experiment because of the above difficulty with  $J \geq 4$  values and because there is indeed some likelihood that for small  $\theta$  at least,  $z_v > 0$  for such substances<sup>2)</sup>. Note that if  $z_v > 0$  below a certain  $\theta = \theta_0$  value and  $z_v = 0$  above it, the present theory with  $J \geq 4$  might apply well for  $\theta > \theta_0$  provided  $\theta_0$  exceeds that  $\theta (\equiv \theta_1)$  at which a pole of  $\Delta V$  could occur. For  $J=8$  and  $R_{1m}=2$ , we find, for example, that the pole still occurs below  $\theta=0.15$ . We even suggest the rough hypothesis, that the  $J \geq 4$  catastrophe makes it energetically more favorable for discrete elements with large  $J$  to be adsorbed initially as adions rather than adatoms, but that it is more favorable for the balance to shift back toward adatoms when  $\theta > \theta_1$ . The situation may be complicated by simultaneous occupation of the surface by adions and adatoms and by possible appreciable variation of  $z_v$  with  $\theta$  for the adions. Finally, we note that even for  $J=3$ ,  $\varepsilon_1(\theta=1) \simeq 5.06$ , by no means a negligible value.

## Appendix

### RATIONAL FUNCTION APPROXIMATIONS

The approximations to  $p(\xi)$  and  $F(\xi)$  are of the form

$$F(\xi) = \sum_{i=0}^n a_i \xi^i / \sum_{i=0}^m b_i \xi^i, \quad (\text{A.1})$$

where  $b_m \equiv 1$ . For the (1/1) approximation  $n=m=1$ , and for the (2/2) approximation  $n=m=2$ . Fitting was generally carried out using 27 accurate values of  $p(\xi)$  or  $F(\xi)$  for the following values of  $\xi$ : 0(0.1)1.6, 1.8(0.2)3.4 and 3.5. Values for  $a_i$  and  $b_i$  for the various cases are given in the following tables. The  $p(\xi)$  approximations given here minimize the absolute value of the relative deviations, while the  $F(\xi)$  approximations were chosen to minimize the absolute value of the absolute deviations. Therefore, values of  $\delta$  included are the maximum relative ( $\delta_R$ ) or absolute ( $\delta_A$ ) errors found between the interpolation formulas and the accurate values of the functions. When a pair of  $\delta$  values appears, that for  $p(\xi)$  is above, that for  $F(\xi)$  below.

TABLE 3  
Coefficients of (1/1) approximations for  $p(\xi)$

$a_i, b_i$	$R_1 = 2$ fit	$R_1 = 5$ fit	$R_1 = \infty$ fit
	$\delta_R = 2.076 \times 10^{-2}$	$\delta_R = 1.939 \times 10^{-2}$	$\delta_R = 1.589 \times 10^{-2}$
$a_0$	2.221 108 9	1.046 724 5	0.690 576 00
$a_1$	0.399 970 32	0.454 063 14	0.473 781 35
$b_0$	3.480 387 0	1.547 614 74	1.007 380 5

TABLE 4  
Coefficients of (2/2) approximations for  $p(\xi)$  and (1/2) approximations for  $F(\xi)$ . Below each coefficient for  $p(\xi)$  the corresponding one for the (1/2) approximation to  $F(\xi)$  appears

$a_i, b_i$	$R_1 = 2$ fit	$R_1 = 5$ fit	$R_1 = \infty$ fit
	$\delta_R = 1.645 \times 10^{-3}$	$\delta_R = 7.314 \times 10^{-4}$	$\delta_R = 5.432 \times 10^{-4}$
	$\delta_A = 8.606 \times 10^{-3}$	$\delta_A = 5.608 \times 10^{-3}$	$\delta_A = 5.857 \times 10^{-3}$
$a_0$	1.020 396 6	0.636 252 04	0.545 216 09
	0	0	0
$a_1$	- 0.719 820 08	- 0.293 762 15	- 0.224 246 08
	0.036 038 417	0.051 641 230	0.053 743 815
$a_2$	0.545 881 0	0.534 402 21	0.532 336 15
	0	0	0
$b_0$	1.634 799 4	0.977 354 54	0.830 499 18
	1.354 542 7	0.874 933 23	0.781 112 58
$b_1$	- 1.201 802 2	- 0.461 050 47	- 0.349 785 27
	- 2.090 217 0	- 1.502 407 5	- 1.382 874 9

## References

- 1) C. A. Barlow, Jr. and J. R. Macdonald, *J. Chem. Phys.* **43** (1965) 2575. The quantities denoted by  $\psi_a(Z)$  and  $\mathcal{E}_a(Z)$  in this reference are here termed  $\psi_{Na}$  and  $\mathcal{E}_a$ .
- 2) J. R. Macdonald and C. A. Barlow, Jr., *J. Chem. Phys.* **44** (1966) 202.
- 3) J. R. Macdonald and C. A. Barlow, Jr., *J. Appl. Phys.*, to be published.
- 4) J. R. Macdonald and C. A. Barlow, Jr., *Can. J. Chem.* **43** (1965) 2985.
- 5) J. Topping, *Proc. Roy. Soc. (London)* **A114** (1927) 67.
- 6) B. M. E. Van der Hoff and G. C. Benson, *Can. J. Phys.* **31** (1953) 1087.
- 7) A. R. Miller, *Proc. Cambridge Phil. Soc.* **42** (1946) 292.
- 8) J. R. Macdonald and C. A. Barlow, Jr., *J. Chem. Phys.* **39** (1963) 412. An error in part of this work is corrected in ref. <sup>3</sup>) above.
- 9) D. C. Grahame, *Z. Elektrochem.* **62** (1958) 264.
- 10) S. Levine, D. Calvert and G. M. Bell, *Nature* **191** (1961) 699.
- 11) N. F. Mott and R. J. Watts-Tobin, *Electrochim. Acta* **4** (1961) 79.
- 12) S. Levine, G. M. Bell and D. Calvert, *Can. J. Chem.* **40** (1962) 518.
- 13) S. Levine, J. Mingins and G. M. Bell, *Can. J. Chem.* **43** (1965) 2834.
- 14) C. A. Barlow, Jr. and J. R. Macdonald, in: *Advances in Electrochemistry and Electrochemical Engineering*, Ed. P. Delahay, to appear.
- 15) J. R. Macdonald, *J. Appl. Phys.* **35** (1964) 3034.
- 16) L. W. Swanson and R. Gomer, *J. Chem. Phys.* **39** (1963) 2813.
- 17) L. D. Schmidt, Ph. D. Dissertation, University of Chicago, Chicago, Ill. (1964).

- 18) J. R. Macdonald and C. A. Barlow, *Symposium on Electrode Reactions, Electrochemistry Society meeting, Cleveland, Ohio, May, 1966*. To be published in J. Electrochem. Soc.
- 19) J. H. De Boer, *Electron Emission and Adsorption Phenomena* (Cambridge University Press, Cambridge, England, 1935) p. 35.
- 20) L. Pauling, *The Nature of the Chemical Bond and the Structure of Molecules and Crystals*, 3rd ed. (Cornell University Press, Ithaca, New York, 1960) p. 403.
- 21) R. M. Sternheimer, *Phys. Rev.* **127** (1962) 1220.
- 22) L. Schmidt and R. Gomer, *J. Chem. Phys.* **42** (1965) 3573.